

# FocusDET, A New Toolbox for SISCOM Analysis. Evaluation of the Registration Accuracy Using Monte Carlo Simulation

Berta Martí Fuster · Oscar Esteban · Xavier Planes · Pablo Aguiar · Cristina Crespo · Carles Falcon · Gert Wollny · Sebastià Rubí Sureda · Xavier Setoain · Alejandro F. Frangi · Maria J. Ledesma · Andrés Santos · Javier Pavía · Domènec Ros

Published online: 19 August 2012  
© Springer Science+Business Media, LLC 2012

**Abstract** Subtraction of Ictal SPECT Co-registered to MRI (SISCOM) is an imaging technique used to localize the epileptogenic focus in patients with intractable partial epilepsy. The aim of this study was to determine the accuracy

of registration algorithms involved in SISCOM analysis using FocusDET, a new user-friendly application. To this end, Monte Carlo simulation was employed to generate realistic SPECT studies. Simulated sinograms were

B. Martí Fuster · C. Crespo · C. Falcon · D. Ros (✉)  
Unitat de Biofísica i Bioenginyeria,  
Departament de Ciències Fisiològiques I, Facultat de Medicina,  
Universitat de Barcelona-IDIBAPS,  
C/Casanova 143 – Planta 5 (Ala Nord),  
E08036 Barcelona, Spain  
e-mail: dros@ub.edu

B. Martí Fuster  
e-mail: bmarti@ub.edu

C. Crespo  
e-mail: ccvaz@hotmail.com

C. Falcon  
e-mail: cfalcon@clinic.ub.es

B. Martí Fuster · O. Esteban · X. Planes · C. Falcon · G. Wollny · A. F. Frangi · M. J. Ledesma · A. Santos · J. Pavía · D. Ros  
Centro de Investigación Biomédica en Red en Bioingeniería,  
Biomateriales y Nanomedicina (CIBER-BBN),  
Campus Río Ebro – Edificio I+D Bloque 5,  
1ª planta C/Poeta Mariano Esquillor s/n,  
E50018 Zaragoza, Spain

O. Esteban  
e-mail: oesteban@die.upm.es

X. Planes  
e-mail: xavier.planes@upf.edu

G. Wollny  
e-mail: gert@die.upm.es

A. F. Frangi  
e-mail: alejandro.frangi@upf.edu

M. J. Ledesma  
e-mail: mledesma@die.upm.es

A. Santos  
e-mail: andres@die.upm.es

J. Pavía  
e-mail: jpavia@clinic.ub.es

O. Esteban · G. Wollny · M. J. Ledesma · A. Santos  
Biomedical Image Technologies,  
Departamento de Ing. Electrónica, ETSI Telecomunicación,  
Universidad Politécnica de Madrid,  
Av. Complutense s/n (Lab. C203),  
E28040 Madrid, Spain

X. Planes · A. F. Frangi  
Center for Computational Imaging and Simulation Technologies  
in Biomedicine (CISTIB), Information and Communications  
Technology Department, Universitat Pompeu Fabra,  
C/Tanger 122-140,  
E08018 Barcelona, Spain

P. Aguiar  
Servizo de Medicina Nuclear, Fundación IDICHUS, Complejo  
Hospitalario Universitario de Santiago de Compostela,  
Rúa da Choupana s/n,  
E15706 Santiago de Compostela, Spain  
e-mail: pablo.aguiar@usc.es

S. Rubí Sureda · X. Setoain · J. Pavía  
Servei de Medicina Nuclear, Hospital Clínic, IDIBAPS,  
C/Villaruel 170,  
E08036 Barcelona, Spain

S. Rubí Sureda  
e-mail: s.rubi.sureda@gmail.com

X. Setoain  
e-mail: setoain@clinic.ub.es

reconstructed by using the Filtered BackProjection (FBP) algorithm and an Ordered Subsets Expectation Maximization (OSEM) reconstruction method that included compensation for all degradations. Registration errors in SPECT-SPECT and SPECT-MRI registration were evaluated by comparing the theoretical and actual transforms. Patient studies with well-localized epilepsy were also included in the registration assessment. Global registration errors including SPECT-SPECT and SPECT-MRI registration errors were less than 1.2 mm on average, exceeding the voxel size (3.32 mm) of SPECT studies in no case. Although images reconstructed using OSEM led to lower registration errors than images reconstructed with FBP, differences after using OSEM or FBP in reconstruction were less than 0.2 mm on average. This indicates that correction for degradations does not play a major role in the SISCOM process, thereby facilitating the application of the methodology in centers where OSEM is not implemented with correction of all degradations. These findings together with those obtained by clinicians from patients via MRI, interictal and ictal SPECT and video-EEG, show that FocusDET is a robust application for performing SISCOM analysis in clinical practice.

**Keywords** Epilepsy · SISCOM · Monte Carlo simulation · Reconstruction algorithms · Registration assessment

## Introduction

Intractable partial epilepsy is a kind of seizure disorder encountered in patients with epilepsy, one of the most common chronic neurological diseases. Partial seizures are focal at onset, which means that they emerge from a localized region of the brain. In addition, more than 30 % of patients with partial seizures are refractory to antiepileptic drug medication (Berg 2008). These two features, focal localization of epileptogenic region and drug resistance, lead us to consider surgery as a possible treatment.

An accurate localization of epileptogenic focus (EF) in intractable partial epilepsy is essential to guarantee success in surgical treatment. To this end, a variety of multimodal techniques including EEG, MRI, SPECT and PET are employed. Ictal SPECT is still the only imaging modality that allows us to assess cerebral blood flow during a seizure without artifacts (Setoain et al. 2012). One of the techniques to analyze ictal SPECT is the Subtraction of Ictal SPECT Co-registered to MRI (SISCOM) (O'Brien et al. 1998a). Several authors agree that this methodology is very useful above all when there is no anatomical lesion and in cases where invasive video-EEG should be avoided (O'Brien et al. 1998b; Vera et al. 1999; Ahnlide et al. 2007; Tan et al. 2008; Matsuda et al. 2009).

SISCOM processing is commonly divided into four steps: SPECT-SPECT (S-S) registration, intensity normalization, subtraction and SPECT-MRI (S-M) registration. To

perform SISCOM analysis, there are computer-aided methods such as those of general purpose in image processing (Acton and Friston 1998; Smith et al. 2004) or those that integrate a SISCOM analysis tool in a larger image software package (Robb and Hanson 1990; Papademetris et al. 2001) which are mainly addressed to researchers or image technicians rather than to clinicians.

This paper presents a multimodal application designed to aid clinicians in the analysis of intractable partial epilepsy. The application named FocusDET (focus detection) allows us to perform the SISCOM analysis by means of a user-friendly interface. The registration algorithms of FocusDET (S-S and S-M) were evaluated by assessing the accuracy of the localization of the EF. We also evaluated the relationship between registration errors and image corrections by reconstructing simulated studies using two reconstruction methods (with and without corrections).

## Materials and Methods

### FocusDET: SISCOM Analysis Tool

The development of this medical application is based on GIMIAS v1.3.0 (Larrabide et al. 2009), a workflow oriented framework for the Biomedical imaging and modelling of prototypes in the context of the Virtual Physiological Human. It is an open source framework distributed under a BSD license, developed in C++ and it is based on robust open source libraries such as VTK, ITK, MITK, DCMTK, NETGEN and TETGEN among others. The main steps to perform SISCOM analysis with FocusDET are described below.

### *Importing Image Files in DICOM from a PACS Server*

To import image files to process the SISCOM analysis, FocusDET provides a PACS server connection via DICOM plug-in. This plug-in allows the user to explore and load DICOM files, including orientation control. Apart from the DICOM format, FocusDET also supports reading and writing of the following formats: vtk, stl, nifti and analyze.

### *Registration of Ictal and Interictal SPECT Studies (S-S)*

To improve the robustness of registration, SPECT studies are masked before this process. To this end, each SPECT study is spatially normalized to a SPECT template by using an affine registration scheme. Subsequently, the inverse transform is applied to a mask manually defined by an expert on the template. Extra-cerebral areas showing significant differences between SPECT studies can be easily removed with the mask.

The registration of SPECT images is performed by using a voxel-based registration algorithm developed earlier

(Pavia et al. 1994; Ros et al. 1999). Registration of the images is carried out by optimizing the value of a cost function in an iterative process which employs the downhill simplex algorithm (Nelder and Mead 1965). The Local Correlation Coefficient (LCC) was the cost function selected (Ros et al. 1999). Briefly, the LCC is defined as the correlation coefficient between both SPECTs around each voxel, calculated in a mask of  $5 \times 5 \times 5$  voxels. The registration algorithm calculates the LCC around each voxel and maximizes the mean of this distribution.

#### *Subtraction of Ictal and Interictal SPECT Files*

In order to minimize total brain count differences between ictal and interictal SPECT studies, intensity normalization is performed before the subtraction process. First, the distribution of quotients between ictal and interictal count values is calculated. Second, a parabola is fitted around the maximum value of the distribution of quotients. The maximum of the parabola is taken as the normalization factor and applied to the interictal study.

A parametric subtraction image,  $S_i$ , containing the relative difference between ictal and interictal image values is obtained. The value  $S_i$  of each voxel  $i$  of this subtraction image, is calculated as:

$$S_i = (I_i - II_i) \cdot 100 / II_i \quad (1)$$

where  $I_i$  and  $II_i$  are  $i$  voxel value of the ictal and interictal studies, respectively. The subtraction image is processed as is indicated in “Fusion of EF Information with MRI” to aid the EF localization.

#### *Generation of a MRI Mask to Extract the Brain Region*

In order to obtain an exact brain mask, a semi-automatic segmentation scheme is performed on the MRI reference. A fuzzy c-means clustering (Pham and Prince 1999) into three classes, followed by the binarization of the class corresponding to white matter is applied. Then, connected components are labeled to finally select the largest one as the white matter. This mask is grown to include the whole brain, the cerebellum and the brain stem. In FocusDET, the user can modify the default parameters of the number of classes (from 3 to 5), the label of white matter class (from 2 to 4) and the intensity threshold governing the growing process. This mask is used to eliminate extracerebral activity on the EF result. The free software implementation of the algorithm is available by Wollny et al. (2012).

#### *Co-Registration of SPECT and MRI Studies (S-M)*

The co-registration of interictal SPECT to MRI reference is performed with a multi-resolution rigid registration scheme

(Studholme et al. 1997), using linear interpolation and implemented over ITK (Insight Image Registration and Segmentation Toolkit (Yoo et al. 2002)).

Pre-processing and initialization: owing to the high diversity of SPECT and MRI intensity distributions, a pre-processing step is required to enhance the features of both images to be registered. Thereafter, for each of the multi-resolution levels data is generated from a smoothed version of the equalized image. The smoothing Gaussian kernel is wider at the lowest level of resolution. The initialization is calculated as the translation between the centers of mass of the two binarized versions of the images, which were obtained by thresholding above quantiles of histogram around the median (65 % for MRI and 50 % for SPECT). In cases when the brain mask of MRI is available (it is generally computed in a previous step of SISCOM analysis), then it is binarized and directly supplied to this initialization (there is no further use of this mask during registration).

Registration process: after the initialization, two levels of multiresolution registration are performed. The lower resolution level is characterized by using Normalized Mutual Information (NMI) metric to evaluate the fitness of the transformation, using the SPSA (Spall 1998) algorithm as optimizer, increasing robustness and capture range efficiently. The processing at full resolution uses the Mutual Information implementation by Mattes et al. (2003) with a modified Gradient Descent optimization, refining the solution of the previous level with minimal cost.

Once the transform matrix of interictal SPECT to MRI is obtained, the mapping of the ictal SPECT and that of the subtraction data to the MRI reference is carried out.

#### *Fusion of EF Information with MRI*

Before the fusion of the EF with the structural 3D MRI, the standard-deviation of the subtraction image values is calculated. Then, the subtraction image is thresholded to generate a new image with values of voxels greater than two standard deviations above zero. This thresholded image is finally merged with the MRI data.

#### *Hardware Requirements*

FocusDET is available for Microsoft Windows XP (x86 and x64) and later. System requirements can be consulted in GIMIAS web site.

#### *Evaluation of Registration Processes of FocusDET*

Monte Carlo (MC) simulation was employed to generate realistic data sets of SPECT projections from a 40 healthy MRI. This strategy introduced anatomical variability into our work and enabled us to evaluate the registration

methods in a well-controlled framework where the ground truth is known (Grova et al. 2003).

Registration errors in SISCOM result in the misallocation of the EF. In order to minimize these errors, S-S and S-M registration methods in SISCOM were optimized by selecting the appropriate values of the registration parameters. The MC simulations, reconstruction algorithms and quantification methods employed to assess the accuracy of the registration algorithms are described below.

### Numerical Brain Maps

The phantom generation was described in detail in a previous work (Aguilar et al. 2008). Briefly, 40 ictal and interictal SPECT studies were simulated by using high-resolution T1-weighted MRI ( $256 \times 256 \times 116$  matrix size;  $0.9375 \times 0.9375 \times 1.5$  mm<sup>3</sup> voxel size), which were segmented into grey matter, white matter and cerebrospinal fluid to obtain activity distribution maps. The attenuation maps were generated from a CT image acquired from an anthropomorphic striatal phantom.

To simulate the ictal studies, epileptogenic foci (EFs) were defined (with volumes from 8.6 to 10.4 cm<sup>3</sup>) by a nuclear-medicine physician expert in nine usual focal regions in intractable partial epilepsy: frontal cortex, occipital cortex, parietal cortex, temporal cortex, hippocampus and amygdala, hippocampus and parahippocampus, insular cortex and orbitofrontal cortex (Lüders 2008). The EF for each subject was obtained by randomly selecting one of the nine and then multiplying it by a randomly generated factor (0.5–0.9) and smoothing it by using a Gaussian filter with a full width at half maximum (FWHM) of 5 mm.

To mimic a real environment, the ictal and interictal maps were misaligned with respect to each other. In translations, three-dimensional displacements between –12 and 12 mm were considered. The rotations were performed around x, y and z image axes in a range of –12 to 12°. Trilinear interpolation was used.

### Simulation

SimSET v2.9 Monte Carlo code (Haynor et al. 1991) was employed to simulate the SPECT projections using the maps described above. SimSET was configured to generate emission projections using <sup>99m</sup>Tc-HMPAO as a radiotracer and a dual detector hybrid SPECT/CT imaging system based on Infinia™ Hawkeye™ 4 from GE Healthcare as a scanner. A parallel collimator with hexagonal holes (radius: 0.75 mm, septal thickness: 0.2 mm) and 35 mm of length was considered. One hundred and twenty projections over 360° ( $128 \times 54$  matrix size;  $3.32 \times 3.32$  mm<sup>2</sup> pixel size) were simulated using a 20 % energy window centered at 140 keV.

The ictal and interictal projections of each study were simulated with a number of photons between 4 and 6 million.

### Reconstruction

Simulated projections were reconstructed by using the Filtered BackProjection (FBP) algorithm, and an Ordered Subsets Expectation Maximization (OSEM) based algorithm (Hudson and Larkin 1994). Both reconstruction methods are recommended in clinical practice (Kapucu et al. 2009), the use of FBP reconstruction being more widespread. However, it is expected, that the use of images free of degradation effects results in an accurate S-M registration, thereby providing an accurate positioning of EF. Thus, OSEM with corrections of the degradations was the second reconstruction method selected.

In FBP reconstruction algorithm, ictal and interictal projections were filtered by using a two-dimensional Butterworth filter (order of filter: 5.8) before reconstruction. Five cut-off frequencies (0.25, 0.50, 0.75, 1.00, 1.25 and 1.50 cm<sup>-1</sup>) were used, last one being the Nyquist frequency  $f_N = 1.50$  cm<sup>-1</sup>. Then, a FBP algorithm using a ramp filter was employed.

In the iterative reconstruction (OSEM), the degrading phenomena such as scatter, attenuation and spatially variant point spread function (PSF) were corrected. Ideal scatter correction was applied by using only non-scattered photons in the sinograms. The attenuation and PSF corrections were included in the reconstruction matrix. The OSEM reconstruction was performed by employing 8 subsets and 2, 4, 6, 8 and 10 iterations per subset.

All images were reconstructed using a matrix of  $128 \times 128 \times 54$  voxels with a voxel size of  $3.32 \times 3.32 \times 3.32$  mm<sup>3</sup>.

### Parameter Optimization

In order to minimize the registration and final EF localization errors, an optimization study was performed to determine the most suitable values of the parameters involved in S-S and S-M registration.

S-S registration parameters: the main parameter that strongly affects this registration is the tolerance of optimization algorithm (downhill simplex). The iterative process ends when changes in cost function are lower than the defined tolerance. Different values of tolerance ( $1 \cdot 10^{-1}$ ,  $5 \cdot 10^{-2}$ ,  $1 \cdot 10^{-2}$ ,  $1 \cdot 10^{-3}$ ,  $1 \cdot 10^{-4}$  and  $1 \cdot 10^{-5}$ ) were tested in order to obtain the relationship between this parameter and the registration error, taking into account the balance between the registration error and the processing time.

S-M parameters: multimodal registration is strongly affected by a number of parameters (Zhu and Cochoff 2002). In order to improve registration accuracy and to reduce

registration time, we conducted a study of two meaningful parameters: smoothing kernel width and number of spatial samples. In the implementation of FocusDET, a discrete Gaussian filtering is performed to reduce the noise of the images and to increase the similarity between registered features. The relationship between registration accuracy and the Gaussian kernel width was assessed using standard deviations in the range of 0–10 mm. As for the number of spatial samples used to compute the cost function (Mattes et al. 2003), this plays an important role in the registration accuracy. A number of samples in the range of 2,000–100,000 were employed to determine the minimum value of samples that guarantee a small registration error and a low computing burden.

#### Assessment of Registration Errors

Registration errors were estimated by comparing the theoretical and experimental geometric transforms obtained during SISCOM analysis. Applying these geometric transforms to an image point, two new points were obtained. The distance between these new points gives an idea of the registration error committed in the registration process. The average of these errors computed in a set of points was defined as the Registration Error (RE):

$$RE = \frac{1}{N} \sum_i \|T_i(\vec{r}) - T_e(\vec{r})\| \quad (2)$$

where  $\vec{r}$  is the position vector of each voxel of the region and  $T_i$  and  $T_e$  are the theoretical and experimental transforms respectively.

RE depends on the distances of the points from the centre of rotation. Thus, the points that are closer to the centre of rotation yield a smaller error, whereas the farthest points generate a greater error. For this reason, two kinds of errors were calculated, depending on the set of points used in 2: 1) Target Registration Error (TRE): using only six points (target points) on the surface of the brain (Mumcuoglu et al. 2006) to obtain a more general measure of error (worst situation), and 2) Lesion Registration Error (LRE): evaluating RE on points belonging to the clinical region of interest (ROI) to obtain a specific and clinically meaningful measure of error. Figure 1 shows an example of these two kinds of points used to compute RE: target points (A) and lesion points (B).

#### Statistical Analysis

Differences between registration errors obtained using both reconstruction methods (FBP and OSEM) were evaluated by a paired *t*-test or by a Wilcoxon rank sum test when the normality test failed. Furthermore, in order to better understand which reconstruction method provides a more

accurate SISCOM result, the Bland-Altman method was applied (Bland and Altman 2010).

#### Assessment of FocusDET by Clinicians

Even though our work was focused on the evaluation of registration accuracy, the usability of FocusDET and the entire SISCOM process (localization of EFs) were also evaluated by the clinicians.

#### Simulated Studies

Localization of simulated EFs with FocusDET was evaluated by two nuclear medicine physicians who were blinded to EFs localization. The experts were asked to localize the EF (i.e. either right or left: frontal, temporal, parietal, occipital, insula or orbito-frontal) in each of the forty simulated studies.

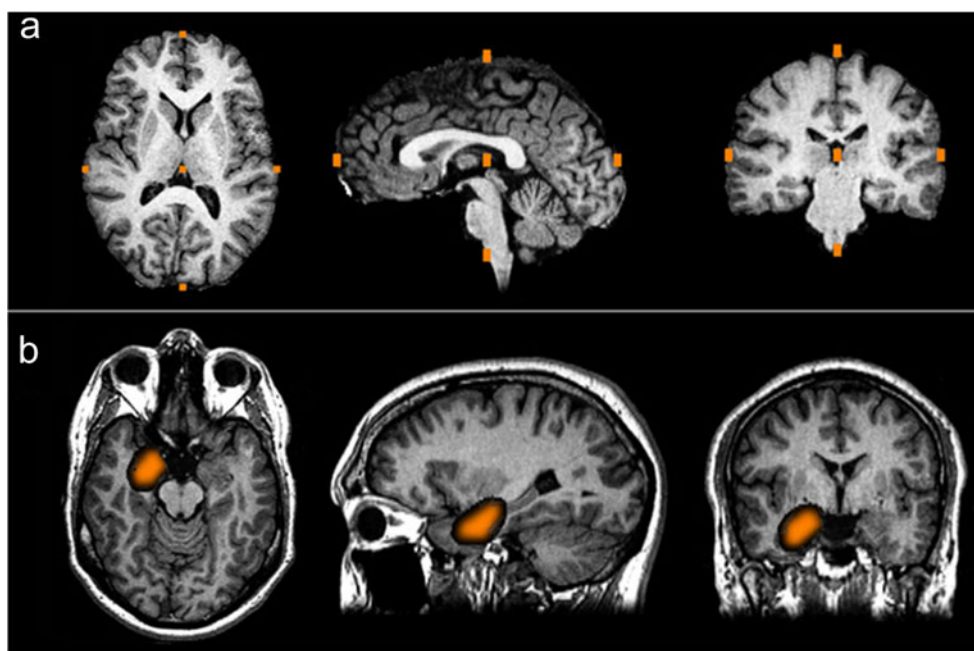
#### Clinical Studies

In order to evaluate FocusDET in a real framework, where physiological differences in regional cerebral blood flow can exist, ten anonymized studies from the Epilepsy Unit database of the Hospital Clinic of Barcelona were selected. The criteria for patient selection were: 1) a lesional MRI and a video-EEG with an agreement in the localization of lesion and seizure onset, and 2) the availability of ictal and interictal SPECT studies and T1-weighted MRI.

Acquisition features of selected data: ictal and interictal studies were acquired within two hours after injection of  $^{99m}\text{Tc}$ -HMPAO (925 MBq), using a dual-head SPECT imaging system (Infinia™ Hawkeye™ 4 from GE Healthcare) with low energy high resolution parallel-hole collimators. The radius of rotation was 14 cm and 120 projections were acquired over 360° at 40 s/projection in a 128×128 matrix with a pixel size of 3.32×3.32 mm<sup>2</sup>. Images were reconstructed using the filtered backprojection algorithm with a Butterworth filter ( $f=0.42\text{ cm}^{-1}$ ; order 5.8) in a same matrix size. T1-weighted MRI studies were performed in a 3T unit (Trio SIEMENS) with a specific protocol: Coronal 3D MPRAGE (TR 2,000 ms; TE 2.98 ms, 0.9 mm slice thickness). The sequence was acquired parallel to the long axis of hippocampus and the full brain was covered.

SISCOM analysis was performed with the aid of FocusDET and an expert, blinded to any information of the patient, indicated his approval (or otherwise) of the registrations carried out. This assessment was performed by a visual evaluation aided by check-registration tools implemented in FocusDET, which consist of an alternate visualization of ictal and interictal studies with a user-editable frequency of change for S-S registration assessment and an overlay of interictal SPECT and MRI studies with user-editable visual

**Fig. 1** Axial, sagittal and coronal views showing the set of points used to obtain the registration errors: target points (a) and lesion points of one of the epileptogenic foci defined (b)



properties (opacity, contrast, lookup tables, zooms, different views and orientations,...) for S-M registration assessment.

The expert also reported the localization of EF (same localization options as for simulations) which was compared with those reported by the neurologist and the neuroradiologist from the video-EEG and MRI, respectively. Epilepsy MRI protocol is detailed by Setoain et al. (2012). Based on the experience of the Epilepsy Unit of Hospital Clinic and other authors, an agreement between lesional MRI and the video-EEG is a guarantee of a successful surgical outcome (Engel et al. 1975; Jack et al. 1992; Jack 1993; Berkovich et al. 1998; O'Brien et al. 1998b). Consequently, SISCOM analysis was considered to be correct when agreeing with the other two techniques.

## Results

### Evaluation of Registration Processes of FocusDET

#### Simulation and Reconstruction

Figure 2 shows examples of activity (A) and attenuation (B) maps used in the simulation, a FBP reconstructed image with cut-off frequency of  $0.75 \text{ cm}^{-1}$  (C) and an OSEM reconstructed image with 8 iterations and 8 subsets with compensation for scatter, attenuation and PSF (D).

#### Parameter Optimization

S-S registration parameters: a total of 2,640 registrations for the 40 studies reconstructed in 11 different conditions (6

cut-off frequencies for FBP and 5 numbers of iterations for OSEM) were performed to test 6 values of tolerance of the downhill simplex algorithm. Figure 3a shows the values of the mean of TRE ( $\mu_{\text{TRE}}$ ) and of processing time ( $\mu_t$ ) against tolerance employed in registration algorithm using images reconstructed by FBP with cut-off frequency of  $0.75 \text{ cm}^{-1}$  and by OSEM with eight iterations and eight subsets. As shown below, both conditions of reconstruction were those for which TRE reached a minimum. The results exhibit the expected behavior, i.e. RE decreased with tolerance. An opposite behavior is observed between processing time and tolerance. For all cases, the minimum error was obtained when a tolerance of  $1 \cdot 10^{-5}$  was used. However, the value of tolerance representing a tradeoff between TRE and processing time is  $1 \cdot 10^{-3}$  in all the registrations performed. Thus, when a tolerance of  $1 \cdot 10^{-3}$  was employed, the processing time was reduced by 60 % at the expense of an increase of 2.3 % in RE.

S-M registration parameters: a total of 1,280 co-registrations for the 40 studies reconstructed with FBP (cut-off frequency of  $0.75 \text{ cm}^{-1}$ ) and OSEM (8 iterations) were performed to test the different number of spatial samples for metric computation ( $40 \text{ studies} \times 2 \text{ reconstructions} \times 7 \text{ values for number of samples}$ ), and the standard deviations for the Gaussian blurring kernel ( $40 \times 2 \times 9 \text{ values for deviation}$ ). Figure 3b and c summarize this performance benchmark. Figure 3b shows an almost-linear increase in computation time with respect to the number of spatial samples used. The mean TRE ( $\mu_{\text{TRE}}$ ) rapidly reaches a minimum of around 1.0 mm using a number of samples above 10,000 for both reconstruction methods. With the aim of keeping the maximum TRE below SPECT studies pixel size (around

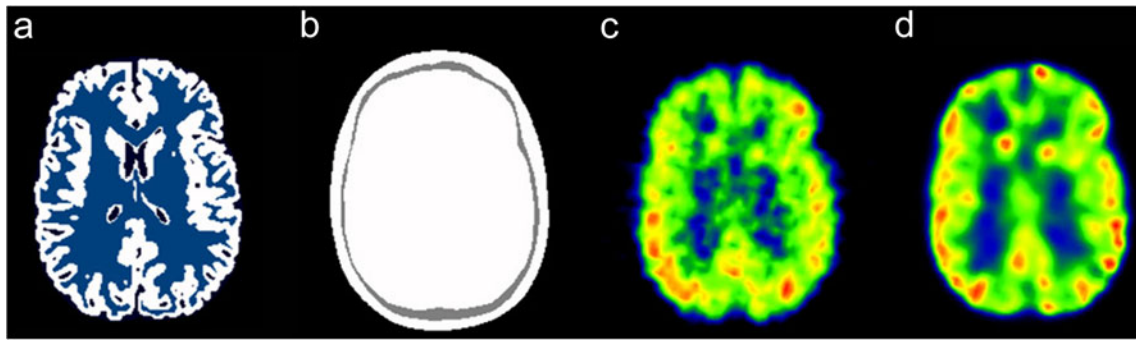


**Fig. 2** Axial views of the 40th-subject of: Activity map (a), Attenuation map (b) and images reconstructed by using FBP (c) and OSEM (d)

3.0 mm), we fixed the number of samples to a secure value of 50,000 samples, resulting in a mean registration time of around 4 min. Figure 3c shows how the kernel width of the blurring filter affects registration accuracy. Small changes of mean TRE in the interval 1.0–1.4 mm are observed and, as a consequence, the standard deviation was selected, looking for a trade-off between maximum TRE and mean registration time. Thus, a standard deviation of 4.0 mm was the most suitable choice for the two reconstruction methods.

#### Assessment of Registration Errors

**FBP Optimization:** Fig. 4a shows the mean LRE against the cut-off frequency of the 2D-Butterworth filter used for pre-filtering the projections. Registration error in S-S registration is almost constant between  $f=0.25 \text{ cm}^{-1}$  and  $f=0.60 \text{ cm}^{-1}$  with a minimum error when  $f=0.50 \text{ cm}^{-1}$ . The minimum error of S-M registration and SISCOM process (combination of S-S registration and S-M registration) is reached when  $f=0.75 \text{ cm}^{-1}$ . The processing time to perform a FBP reconstruction was around 1 min.

**OSEM Optimization:** Figure 4b shows the mean LRE against iterations. Registration error in S-S registration is almost constant through iterations while the error reaches a minimum using images reconstructed with eight iterations in the S-M registration and SISCOM process. The processing time in OSEM reconstruction was 120 min.

In order to compare the reconstruction methods,  $f=0.75 \text{ cm}^{-1}$  for FBP reconstruction and  $it=8$  for OSEM reconstruction were selected. As Fig. 4 shows, these parameters are those for which SISCOM RE achieved the minimum. Figure 5 shows an axial section of reconstructed images (randomly selected) by using both reconstruction methods. For FBP reconstruction (Fig. 5a), the three images were obtained by using three cut-off frequencies  $f=0.50$ ,  $f=0.75$  and  $f=1.00 \text{ cm}^{-1}$ . For OSEM (Fig. 5b), the images correspond to reconstructions obtained after 6, 8 and 10 iterations.

Table 1 summarizes the registration errors of S-S registration, S-M registration and the final error of SISCOM process

using these values of cut-off frequency and the number of iterations. Mean, standard deviation, minimum and maximum registration errors for the forty studies are shown. In S-S registration a close match between the experimental and theoretical geometric transform was found with the result that LRE and TRE values were less than 1 mm (three times less than voxel size of SPECT studies  $-3.32 \text{ mm}$ ) for the two reconstruction methods. In S-M registration the registration errors were less than 2 mm for the two methodologies, LRE and TRE. The errors found on SISCOM process were similar to S-M registration, with errors less than 1.20 mm on average for all methods. The registration errors generated by using OSEM reconstruction are less than those obtained when FBP reconstruction is employed, regardless of the method employed to calculate RE, in all the processes evaluated.

#### Statistical Analysis

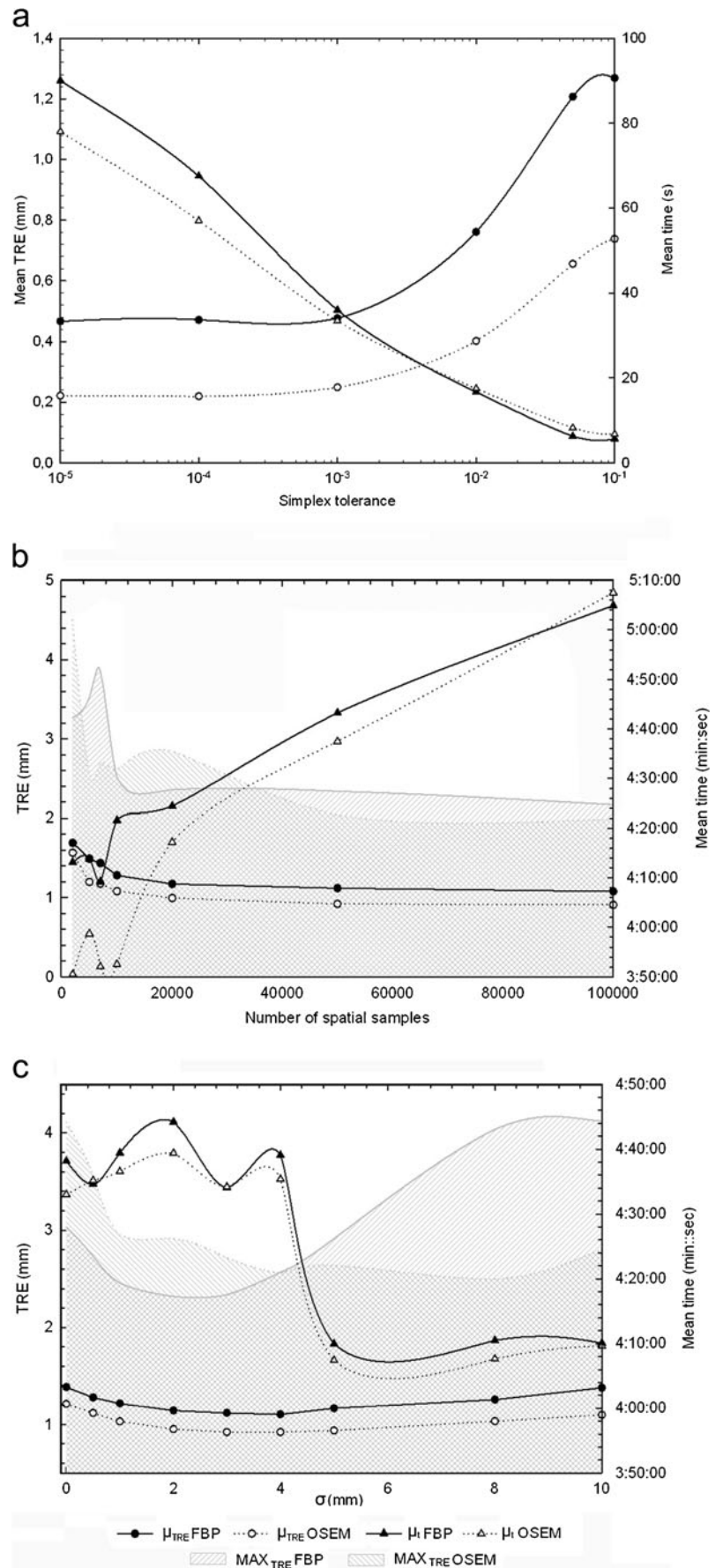
LRE and TRE were significantly lower in the S-S registration ( $p<0.01$ ) and in the S-M registration ( $p<0.01$  for LRE and  $p<0.05$  for TRE) when OSEM rather than FBP reconstruction was employed (Table 1). Figure 6 shows a Bland-Altman plot of the differences in TRE (A) and LRE (B) when FBP or OSEM were employed against the mean responses of registration errors of the two methods. No relationship between these two variables is observed. The mean bias of 0.19 mm in TRE and 0.12 mm in LRE (solid line in Fig. 6a and b, respectively) quantifies the improvement of the OSEM method with respect to FBP. Dashed lines in both plots in Fig. 6 represent two standard deviations above and below the mean difference constituting a measure of the extent of disagreement between the two methods.

#### Assessment of FocusDET by Clinicians

#### Simulated Studies

The two experts agreed on the localization of EF when FBP reconstructed images were assessed. The agreement of the experts also correlated with the theoretical localization of EF.

**Fig. 3** Optimization of registration parameters. Mean processing time ( $\mu_t$ ) and mean target registration error ( $\mu_{TRE}$ ) vs: **a** tolerance for SPECT-SPECT optimization, **b** spatial samples and **c** standard deviation of Gaussian blurring kernel for SPECT-MRI optimization. Filled symbols and solid lines correspond to FBP reconstructions. Hollow symbols and dotted lines correspond to OSEM reconstructions. Circles and triangles indicate  $\mu_{TRE}$  and  $\mu_t$  respectively. Shaded regions represent maximum values of TRE



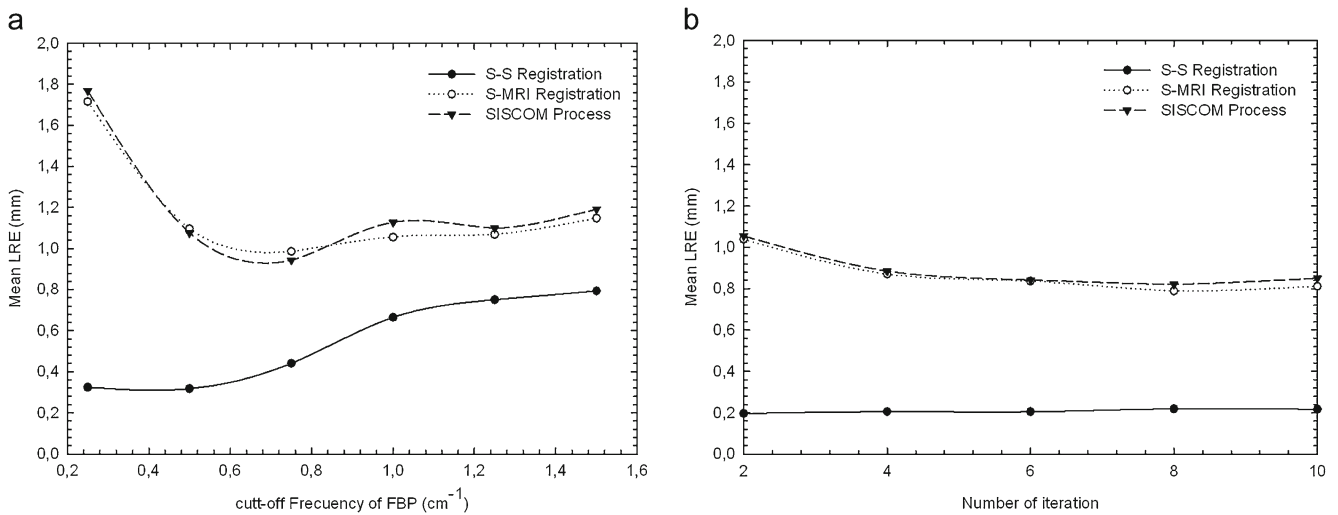


**Fig. 4** Mean lesion registration error (LRE) versus cut-off frequency of the 2D-Butterworth filter used in FBP reconstruction (a) and number of iterations of OSEM reconstruction (b)

*Clinical Studies*

S-S and S-M registrations were considered to be accurate by the expert in all patient studies. In terms of FocusDET functionality, a total agreement between modalities on the localization of EF was found (Table 2). Figure 7 shows an example of SISCOM output evaluated by the expert from a patient.

The two clinicians considered FocusDET as a user-friendly medical application and spent 6 min on average to obtain a SISCOM output. All the results presented above

were obtained by using an Intel<sup>(R)</sup> Core<sup>(TM)</sup>2 Quad CPU Q6600@2.40 GHz 8.00 GB RAM system.

**Discussion**

In the present study, FocusDET, a new application to localize the epileptogenic focus in intractable partial epilepsy using the SISCOM methodology has been presented and evaluated. We assessed the registration errors involved in the SISCOM process by using Monte Carlo SPECT

**Fig. 5** Axial views of the 40th-subject. FBP reconstructed images obtained with cut-off frequencies of 0.50, 0.75 and 1.00  $\text{cm}^{-1}$  (a) and OSEM reconstructed images after 6, 8 and 10 iterations (b)

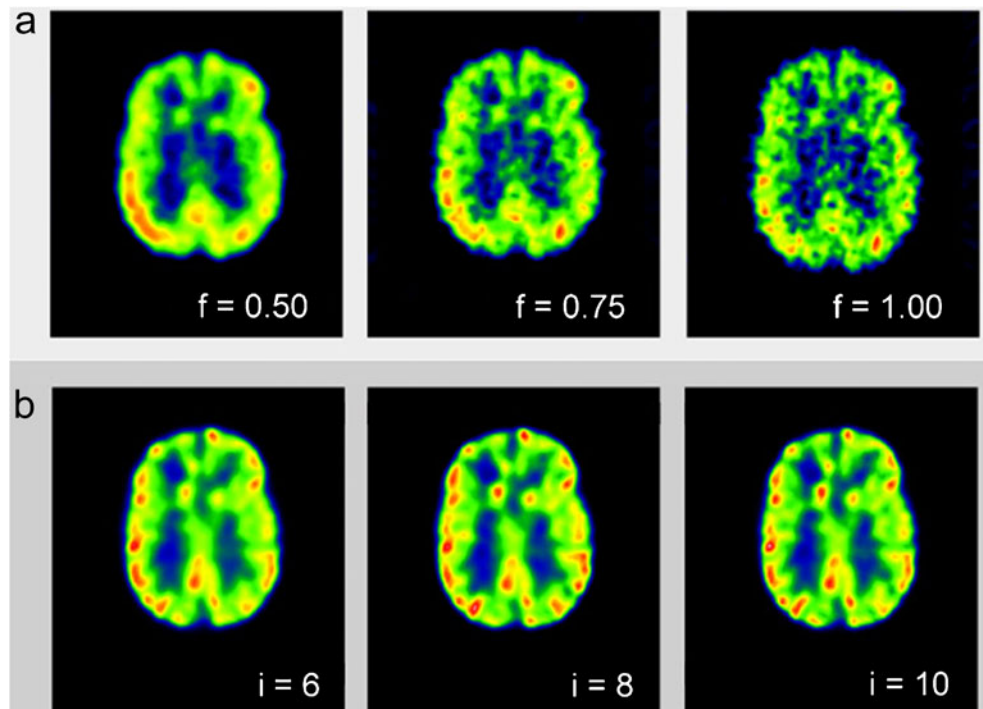


**Table 1** Registration errors (mm) in S-S registration, S-M registration and SISCOM process (S-S registration and S-M registration) of SPECT studies reconstructed by using FBP and OSEM methods

		SS-RE			S-M-RE			SISCOM-RE		
		Mean ( $\pm$ SD)	Min	Max	Mean ( $\pm$ SD)	Min	Max	Mean ( $\pm$ SD)	Min	Max
TRE	FBP	0.48 $\pm$ 0.15	0.23	0.81	1.12 $\pm$ 0.29	0.61	1.67	1.14 $\pm$ 0.28	0.63	1.69
	OSEM	0.25 $\pm$ 0.07	0.11	0.43	0.92 $\pm$ 0.28	0.51	1.54	0.94 $\pm$ 0.26	0.54	1.55
	<i>p</i> value	<0.01*			<0.01**			<0.01**		
LRE	FBP	0.44 $\pm$ 0.18	0.18	0.89	0.99 $\pm$ 0.39	0.17	1.92	0.94 $\pm$ 0.40	0.29	2.25
	OSEM	0.22 $\pm$ 0.10	0.06	0.44	0.79 $\pm$ 0.34	0.30	1.86	0.82 $\pm$ 0.40	0.19	1.99
	<i>p</i> value	<0.01**			<0.05**			N.S		

FBP parameters: cut-off frequency of 0.75 cm<sup>-1</sup> and order of filter 5.8

OSEM parameters: 8 iterations per subset and 8 subsets with scatter, attenuation and PSF correction

*p* value of mean registration errors using FBP vs. OSEM reconstructed images (\*paired *t*-test and \*\*Wilcoxon rank sum test)

simulations, including anatomical variability and epileptogenic foci positioned in several anatomical areas where they are usually located.

In clinical practice, reconstruction of SPECT images is usually performed by using FBP reconstruction with low cut-off frequencies in order to obtain a smooth image, which is useful for visual analysis. Nevertheless, after the results of Fig. 5a, the cut-off frequency recommended for the SISCOM analysis using FBP reconstruction is 0.75 cm<sup>-1</sup> (1/2f<sub>N</sub>). To maintain a suitable signal-to-noise ratio for visual evaluation, a smoothing process of registered images could be applied after the registration process. For OSEM reconstruction, Fig. 5b shows that registration errors in the SISCOM process reaches the minimum after 8 iterations. Although the reconstruction with corrections (OSEM) is increasingly used, the small differences found between both reconstructions methods (with or without corrections) make the use of FBP a suitable method of reconstruction in terms

of registration errors with FocusDET, especially for those centers that do not have the possibility of correcting images for these degrading effects.

SPECT-SPECT registration has been a challenging process because the better the registration, the fewer the artifacts in the final result of SISCOM analysis (Brinkmann et al. 1999). Comparing our findings (Table 1) with the results of other studies, the use of the local correlation coefficient as a cost function yields lower registration errors than other cost functions such as is NMI (Mumcuoglu et al. 2006).

As regards SPECT-MRI registration, our results show the importance of the optimization of the Gaussian kernel width and the number of samples used to compute the cost function. Thus, the registration errors are lower than the voxel size when using the optimum registration parameters and NMI–MMI as the cost functions, and very similar than other studies (Barnden et al. 2000 and Thurfjell et al. 2000).

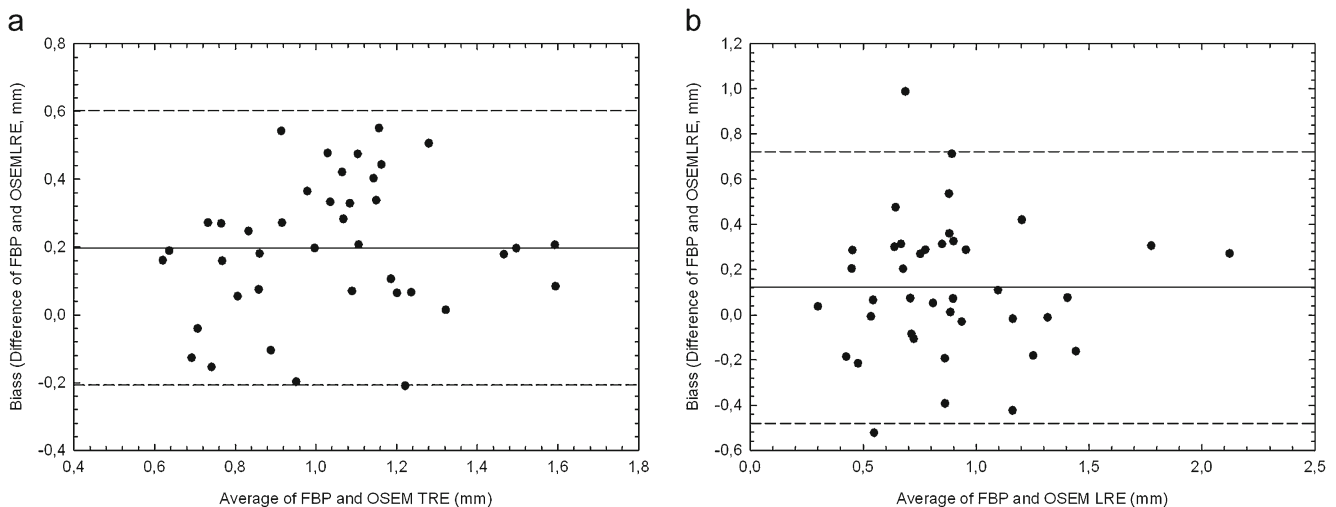


**Fig. 6** Bland Altman plots between SISCOM target registration error (TRE, **a**) and lesion registration error (LRE, **b**) using FBP and OSEM reconstructed images. *Solid line* represents the mean bias and *dashed lines* indicate two standard deviations above and below this mean bias

**Table 2** Comparison of EF localization from video-EEG monitoring, MRI and SISCOM (aided by FocusDET) in patients with partial epilepsy

Patient ID	EEG Ictal	MRI	SISCOM
1	R parietal	R fronto-parietal	R parietal <sup>a</sup>
2	R temporal	R temporal (MTS)	R temporal <sup>a</sup>
3	L temporal	L temporal (MTS)	L temporal <sup>a</sup>
4	L temporal	L temporal (Tu amygdala)	L temporal <sup>a</sup>
5	R temporal	R temporal (MTS)	R temporal <sup>a</sup>
6	L temporal	L temporal (MTS)	L temporal <sup>a</sup>
7	R temporal	R temporal (Tu or Dys)	R temporal <sup>a</sup>
8	R temporal	R temporal (MTS)	R temporal <sup>a</sup>
9	L temporal	L temporal (possible DNET)	L temporal <sup>a</sup>
10	L temporal	L temporal (MTS+Dys L temporal)	L temporal <sup>a</sup>

*MTS* mesial temporal sclerosis; *Tu* tumor; *Dys* dysplasia; *DNET* dysembryoplastic neuroepithelial tumor

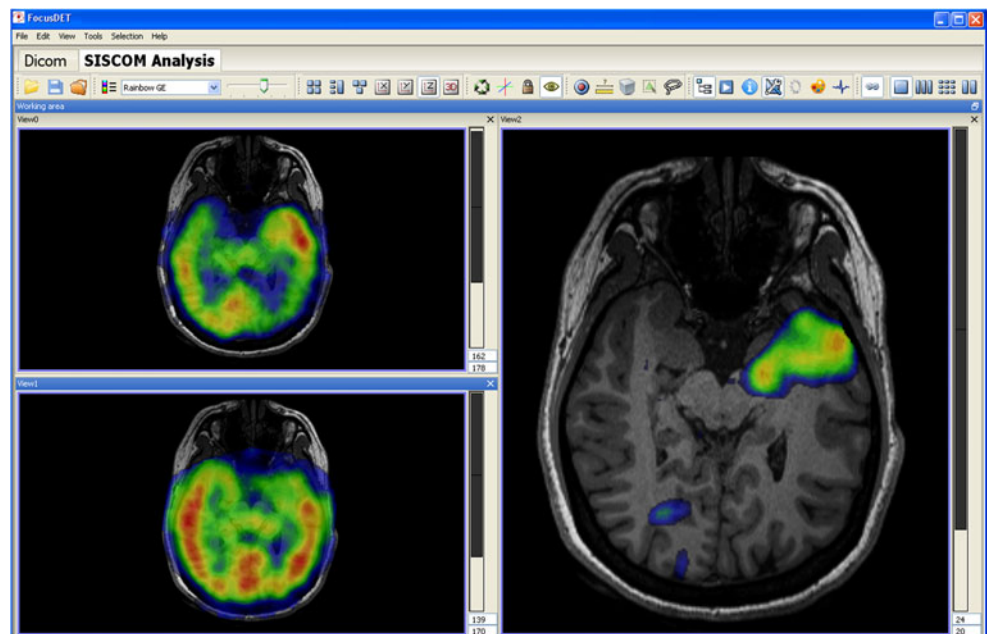
<sup>a</sup>Both registrations methods (S-S registration and S-M registration) approved by the expert clinician

Evaluation of registration algorithms with real cases is always problematic. In epilepsy surgery, where three studies (two SPECTs and MRI) are performed and multimodal registrations are involved, the challenge increases. In this situation, the use of fiducial markers is practically ruled out. Thus, the FocusDET facility described above is considered to be an appropriated visual tool for accepting or discarding a registration. In this way, we take advantage of the expertise of nuclear medicine physicians in evaluating images to assess the accuracy of the registration processes in a qualitative but skilled way. The excellent results obtained in the registration error using simulated studies, and in the qualitative assessment of the registration process by experts using patient studies, support the robustness of FocusDET registration algorithms.

In addition to registration assessment, the qualitative analysis of the epileptogenic focus localizations using simulation

and patient studies allowed us to evaluate the entire SISCOM process. Our results show an agreement in epileptogenic focus localization in simulated studies (between theoretical and reported localizations) and patient cases (between localizations from MRI and video-EEG techniques and that reported by the expert from SISCOM output). For simulation data, false positives were improbable because there are no differences, other than focus and real noise, between ictal and interictal SPECTs. Nevertheless, false positives are likely in the case of patient studies. False positives in partial epilepsy studies have several origins, the most important one being associated with injection latency. In our set of patients, the ictal studies selected are true ictal SPECT, i.e., the tracer injection was performed close to the seizure onset and no propagation artifacts were detected in the SISCOM analysis. Besides, a localization error could be due to a registration error. The agreement between the

**Fig. 7** FocusDET interface. Ictal SPECT (*top left*), interictal SPECT (*bottom left*) and the EF (*right*), all of them are merged with the MRI of the database of the Epilepsy Unit (Hospital Clinic of Barcelona)



different techniques (video-EEG, MRI and SISCOM) in each of patients studied reinforced the impression of a well performed registration given that no propagation was observed a posteriori.

It should also be pointed out that FocusDET registration algorithms have been tested in 62 patients from the Epilepsy Unit database, and the registrations were considered to be satisfactory for the clinicians in every case. These studies have not been included as they do not fulfill the selection criteria required of patients with a well-localized epilepsy, whom we considered as a gold standard for our validation of the localization.

In summary, our findings show that SISCOM analysis with FocusDET led to small registration errors and satisfactory results in the evaluation of experts in both simulated and patient studies.

## Conclusion

SISCOM analysis with the user-friendly FocusDET application is a robust method to localize epileptogenic focus in intractable partial epilepsy. Our findings show that the global registration errors are lower than the voxel size, and that the registration processes of FocusDET are slightly affected by correction of degradations.

## Information Sharing Statement

FocusDET software, information and sample data is freely available in CIBER-BBN website (<http://www.ciber-bbn.es/focusdet>).

**Acknowledgments** This work was supported in part by Virtual Physiological Human Toolkit (VPHTk) project of Centro de Investigación Biomédica en Red en Bioingeniería, Biomateriales y Nanomedicina (CIBER-BBN), by Talència's grants 2009SGR-00866 and 2009SGR-1049, by Ministerio de Ciencia e Innovación (SAF2009-08076), by the European Commission VPH Network of Excellence (IST-2007-223920) and by Spain's Ministry of Science & Innovation through CDTI-CENIT (AMIT project) and project TEC2010-21619-C04-03; Comunidad de Madrid (ARTEMIS S2009/DPI-1802), and the European Regional Development Funds (FEDER). B. Martí was awarded a PhD fellowship (App Form—Call 07-2009) of Institute for Bioengineering of Catalonia (IBEC). A.F. Frangi holds an ICREA-Academia Award from the Institució Catalana de Recerca i Estudis Avançats (ICREA).

## References

Acton, P. D., & Friston, K. J. (1998). Statistical parametric mapping in functional neuroimaging: beyond PET and fMRI activation studies. *European Journal of Nuclear Medicine and Molecular Imaging*, 25, 663–667.

- Aguilar, P., Pareto, D., Gispert, J. D., Crespo, C., Falcon, C., Cot, A., et al. (2008). Effect of anatomical variability, reconstruction algorithms and scattered photons on the SPM output of brain PET studies. *Neuroimage*, 39(3), 1121–1128.
- Ahnlide, J. A., Rosen, I., Tech, P. L. M., & Kallen, K. (2007). Does SISCOM contribute to favorable seizure outcome after epilepsy surgery? *Epilepsia*, 48, 579–588.
- Barnden, L., Kwiatek, R., Lau, Y., Hutton, B., Thurfjell, L., Pile, K., et al. (2000). Validation of fully automatic brain SPET to MR coregistration. *Eur. J. Nucl. Med.*, 27, 147–154.
- Berg, A. T. (2008). Epidemiology of the intractable generalized epilepsies. In H. O. Lüders (Ed.), *Epilepsy surgery* (pp. 207–214). London: Informa healthcare.
- Berkovich, A. J., Berkovic, S. F., Cascino, G. D., Chiron, C., Duncan, J. S., Gadian, D. G., et al. (1998). Guidelines for neuroimaging evaluation of patients with uncontrolled epilepsy considered for surgery. *Epilepsia*, 39, 1375–1376.
- Bland, J. M., & Altman, D. G. (2010). Statistical methods for assessing agreement between two methods of clinical measurement. *International Journal of Nursing Studies*, 47, 931–936.
- Brinkmann, B. H., O'Brien, T. J., Aharon, S., O'Conner, M. K., Mullan, B. P., & Hanson, D. P. (1999). Quantitative and clinical analysis of SPECT image registration for epilepsy studies. *Journal of Nuclear Medicine*, 40, 1098–1105.
- Engel, J., Driver, M. V., & Falconer, M. A. (1975). Electrophysiological correlates of pathology and surgical results in temporal-lobe epilepsy. *Brain*, 98, 129–156.
- Grova, C., Jannin, P., Biraben, A., Buvat, I., Benali, H., Bernard, A. M., et al. (2003). A methodology for generating normal and pathological brain perfusion SPECT images for evaluation of MRI/SPECT fusion methods: application in epilepsy. *Physics in Medicine and Biology*, 48, 4023–4043.
- Haynor, D. R., Harrison, R. L., & Lewellen, T. K. (1991). The use of importance sampling techniques to improve the efficiency of photon tracking in emission tomography simulations. *Medical Physics*, 18, 990–1001.
- Hudson, H. M., & Larkin, R. S. (1994). Accelerated image-reconstruction using ordered subsets of projection data. *IEEE Transactions on Medical Imaging*, 13, 601–609.
- Jack, C. R. (1993). Epilepsy—surgery and imaging. *Radiology*, 189, 635–646.
- Jack, C. R., Sharbrough, F. W., Cascino, G. D., Hirschorn, K. A., O'Brien, P. C., & Marsh, W. R. (1992). Magnetic-resonance image based hippocampal volumetry—correlation with outcome after temporal lobectomy. *Annals of Neurology*, 31, 138–146.
- Kapucu, O. L., Nobili, F., Varrone, A., Booi, J., Vander Borght, T., Nagren, K., et al. (2009). EANM procedure guideline for brain perfusion SPECT using Tc-99m-labelled radiopharmaceuticals, version 2. *European Journal of Nuclear Medicine and Molecular Imaging*, 36, 2093–2102.
- Larrabide, I., Omedas, P., Martelli, Y., Planes, X., Nieber, M., Moya, J. A., et al. (2009). GIMIAS: an open source framework for efficient development of research tools and clinical prototypes. *Functional Imaging and Modeling of the Heart, ser. Lecture Notes in Computer Science*, 5528, 417–426.
- Lüders, H. O. (2008). Classification of epileptic seizures and epilepsies. In H. O. Lüders (Ed.), *Epilepsy surgery* (pp. 245–248). London: Informa healthcare.
- Matsuda, H., Matsuda, K., Nakamura, F., Kameyama, S., Masuda, H., Otsuki, T., et al. (2009). Contribution of subtraction ictal SPECT coregistered to MRI to epilepsy surgery: a multicenter study. *Annals of Nuclear Medicine*, 23, 283–291.
- Mattes, D., Haynor, D. R., Vesselle, H., Lewellen, T. K., & Eubank, W. (2003). PET-CT image registration in the chest using free-form deformations. *IEEE Transactions on Medical Imaging*, 22, 120–128.

- Mumcuoglu, E. U., Nar, F., Yardimci, Y., Kocak, U., Ergun, E. L., Salanci, B. V., et al. (2006). Simultaneous surface registration of ictal and interictal SPECT and magnetic resonance images for epilepsy studies. *Nuclear Medicine Communication*, 27, 45–55.
- Nelder, J. A., & Mead, R. (1965). A simplex-method for function minimization. *Computer Journal*, 7, 308–313.
- O'Brien, T. J., O'Connor, M. K., Mullan, B. P., Brinkmann, B. H., Hanson, D., Jack, C. R., et al. (1998). Subtraction ictal SPET co-registered to MRI in partial epilepsy: description and technical validation of the method with phantom and patient studies. *Nuclear Medicine Communication*, 19, 31–45.
- O'Brien, T. J., So, E. L., Mullan, B. P., Hauser, M. F., Brinkmann, B. H., Bohnen, N. I., et al. (1998). Subtraction ictal SPECT co-registered to MRI improves clinical usefulness of SPECT in localizing the surgical seizure focus. *Neurology*, 50, 445–454.
- Papademetris, X., Jackowski, M., Rajeevan, N., Constable, R. T., & Staib, L. H. (2001). BioImage suite: an integrated medical image analysis suite. Section of Bioimaging Sciences, Dept. of Diagnostic Radiology, Yale School of Medicine. <http://www.bioimagesuite.org>
- Pavia, J., Ros, D., Catafau, A. M., Lomena, F. J., Huguet, M., & Setoain, J. (1994). 3-Dimensional realignment of activation brain single-photon emission tomographic studies. *European Journal of Nuclear Medicine and Molecular Imaging*, 21, 1298–1302.
- Pham, D. L., & Prince, J. L. (1999). An adaptive fuzzy C-means algorithm for image segmentation in the presence of intensity inhomogeneities. *Pattern Recog. Lett.*, 20, 57–68.
- Robb, R. A., & Hanson, D. P. (1990). ANALYZE: a software system for biomedical image analysis. *Proceedings of the First Conference on Visualization in Biomedical Computing*. doi:10.1109/VBC.1990.109363.
- Ros, D., Espinosa, M., Setoain, J. F., Falcon, C., Lomena, F. J., & Pavia, J. (1999). Evaluation of algorithms for the registration of Tc-99(m)-HMPAO brain SPET studies. *Nuclear Medicine Communication*, 20, 227–236.
- Setoain, X., Pavia, J., Seres, E., Garcia, R., Carreno, M. M., Donaire, A., et al. (2012). Validation of an automatic dose injection system for Ictal SPECT in epilepsy. *Journal of Nuclear Medicine*, 53, 324–329.
- Smith, S. M., Jenkinson, M., Woolrich, M. W., Beckmann, C. F., Behrens, T. E. J., Johansen-Berg, H., et al. (2004). Advances in functional and structural MR image analysis and implementation as FSL. *Neuroimage*, 23, S208–S219.
- Spall, J. C. (1998). Implementation of the simultaneous perturbation algorithm for stochastic optimization. *IEEE Transactions on Aerospace and Electronic Systems*, 34, 817–823.
- Studholme, C., Hill, D. L. G., & Hawkes, D. J. (1997). Automated three-dimensional registration of magnetic resonance and positron emission tomography brain images by multiresolution optimization of voxel similarity measures. *Medical Physics*, 24, 25–35.
- Tan, K. M., Britton, J. W., Buchhalter, J. R., Worrell, G. A., Lagerlund, T. D., Shin, C., et al. (2008). Influence of subtraction ictal SPECT on surgical management in focal epilepsy of indeterminate localization: a prospective study. *Epilepsy Research*, 82, 190–193.
- Thurfjell, L., Lau, Y. H., Andersson, J. L., & Hutton, B. F. (2000). Improved efficiency for MRI-SPET registration based on mutual information. *European Journal of Nuclear Medicine*, 27, 847–856.
- Vera, P., Kaminska, A., Cieuta, C., Hollo, A., Stievenart, J. L., Gardin, I., et al. (1999). Use of subtraction ictal SPECT co-registered to MRI for optimizing the localization of seizure foci in children. *Journal of Nuclear Medicine*, 40, 786–792.
- Wollny, G., Ledesma-Carbayo, M.J., Santos, A. (2012). MIA—A toolbox for medical image analysis. *Workshop on open-source medical image analysis software*, Barcelona, Spain. [mia.sourceforge.net](http://mia.sourceforge.net)
- Yoo, T. S., Ackerman, M. J., Lorensen, W. E., Schroeder, W., Chalana, V., Aylward, S., et al. (2002). Engineering and algorithm design for an image processing API: a technical report on ITK—the insight toolkit. *Studies in Health Technology and Informatics*, 85, 586–592.
- Zhu, Y. M., & Cochoff, S. M. (2002). Influence of implementation parameters on registration of MR and SPECT brain images by maximization of mutual information. *Journal of Nuclear Medicine*, 43, 160–166.